
Nonparametric Bayesian Deep Networks with Local Competition

Konstantinos P. Panousis

Dept. of and Informatics and Telecommunications
 National and Kapodistrian University of Athens
 kpanousis@di.uoa.gr

Sotirios Chatzis

Dept. of Electrical Eng., Computer Eng., and Informatics
 Cyprus University of Technology
 sotirios.chatzis@cut.ac.cy

Sergios Theodoridis^{1,2}

¹Dept. of Informatics and Telecommunications
 National and Kapodistrian University of Athens
²The Chinese University of Hong Kong, Shenzhen
 stheodor@di.uoa.gr

Abstract

Local competition among neighboring neurons is a common procedure taking place in biological systems. This finding has inspired research on more biologically plausible deep networks that comprise competing linear units; such models can be effectively trained by means of gradient-based backpropagation. This is in contrast to traditional deep networks, built of nonlinear units that do not entail any form of (local) competition. However, for the case of competition-based networks, the problem of data-driven inference of their most appropriate configuration, including the needed number of connections or locally competing sets of units, has not been touched upon by the research community. This work constitutes the first attempt to address this shortcoming; to this end, we leverage solid arguments from the field of Bayesian nonparametrics. Specifically, we introduce auxiliary discrete latent variables of model component utility, and perform Bayesian inference over them. We impose appropriate stick-breaking priors over the introduced discrete latent variables; these give rise to an well-established sparsity-inducing mechanism. We devise efficient inference algorithms for our model by resorting to stochastic gradient variational Bayes. We perform an extensive experimental evaluation of our approach using benchmark data. Our results verify that we obtain state-of-the-art accuracy albeit via networks of much smaller memory and computational footprint than the competition.

1 Introduction

Deep neural networks (DNNs) [1] are flexible models that represent complex functions as a combination of simpler primitives. Despite their success in a wide range of applications, they typically suffer from overparameterization: they entail millions of parameters, a large fraction of which is actually redundant. This leads to unnecessary computational burden, and limits their scalability to

commodity hardware devices. In addition, this fact renders them susceptible to strong overfitting tendencies that may severely undermine their generalization capacity.

The deep learning community has devoted significant effort to address overfitting in deep learning; ℓ_2 regularization, Dropout, and variational variants thereof are characteristic such examples [2]. However, the scope of regularization is limited to effectively training (and retaining) all postulated model parameters. An alternative path to address redundancy in deep networks would be to adopt data-driven structure shrinkage and parameter compression techniques.

A popular type of solution to this end consists in training a condensed student network by leveraging a previously trained full-fledged teacher network [3, 4]. However, this paradigm suffers from two main drawbacks: (i) One cannot avoid the computational costs and overfitting tendencies related to training a large deep network; on the contrary, the total training costs are augmented with the weight distillation and training costs of the student network; and (ii) the student teaching procedure itself entails a large deal of heuristics and assorted artistry in designing effective teacher distillation.

As an alternative, several researchers have examined application of network component (unit, connection) pruning criteria. In most cases, these criteria are applied on top of some appropriate regularization technique. In this context, Bayesian Neural Networks (BNNs) have been proposed as a full probabilistic paradigm for formulating DNNs [2, 5]. BNNs are obtained by imposing a prior distribution over the weights of DNNs. Then, appropriate posteriors are inferred, and their predictive distribution is obtained via marginalization in the Bayesian averaging sense. This way, BNNs induce strong regularization under a solid inferential framework. In addition, they naturally allow for leveraging sparsity-inducing priors in devising the inference algorithm [6].

Recently, [7] addressed these shortcomings in the context of latent encoding dimensionality inference for variational autoencoders. They introduce an additional set of auxiliary Bernoulli latent variables, which explicitly indicate the utility of each latent direction (in an "on/off" fashion). In this context, they obtain a sparsity-inducing behavior, by imposing appropriate stick-breaking priors [8] over the postulated auxiliary latent variables.

On the other hand, a prevalent characteristic of modern deep networks is the use of nonlinear units on each hidden layer. Even though this sort of functionality offers a mathematically convenient way of creating a hierarchical model, it is also well understood that it does not come with strong biological plausibility. Indeed, there is an increasing body of evidence supporting that neurons in biological systems that have similar functional properties are aggregated together in modules or columns wherein local competition takes place [9–14]. This is effected via the entailed lateral inhibition mechanisms, under which only a single neuron within a block can be active at a steady state. Drawing from this inspiration, several researchers have examined development of deep networks which replace nonlinear units with local competition mechanisms among simpler linear units. As it has been shown, such local winner-takes-all (LWTA) networks can discover effective sparsely distributed representations of their input stimuli [15, 16], and constitute universal function approximators, as powerful as networks with threshold or sigmoidal units [17, 18]. In addition, this type of network organization has been argued to give rise to a number of interesting properties, including automatic gain control, noise suppression, and prevention of catastrophic forgetting in online learning settings [19–21].

This paper draws from these results, and attempts to offer a principled paradigm for regularization and network compression in the context of biologically-inspired LWTA-based deep networks. We posit that the capacity to infer an explicit posterior distribution of component (connection/unit) utility/redundancy in the context of LWTA-based deep networks may offer significant advantages in model effectiveness and computational efficiency. The proposed inferential construction gives rise to a data-driven mechanism that intelligently adapts model structure. Our theoretical expectation is that this mechanism will enable retaining as much model components as barely needed to best model the data at hand. We derive efficient training and inference algorithms for our model, by relying on stochastic gradient variational Bayes (SGVB). We dub our approach Stick-Breaking LWTA (SB-LWTA) networks. We evaluate our approach using well-known benchmark datasets. Our provided empirical evidence vouches for the capacity of our approach to yield predictive accuracy at least competitive with the state-of-the-art, while shrinking model complexity better than the competition, in an intelligent and non-ad-hoc manner.

The remainder of this paper is organized as follows: In Section 2, we briefly present some necessary theoretical background. In Section 3, we introduce the proposed approach, and elaborate on its

training and inference algorithms. In Section 4, we perform an extensive experimental evaluation of our approach, and provide insights into its functionality. Finally, in the concluding Section, we summarize the contribution of this work, and discuss directions for further research.

2 Theoretical Background

2.1 Indian Buffet Process

The Indian Buffet Process (IBP) [22] is a probability distribution over infinite binary matrices. By using it as a prior, it allows for inferring how many features are needed for modeling a given set of observations, in a way that ensures sparsity in the obtained representations. In addition, it also allows for the emergence of new features as new observations appear. Teh et al. [23], presented a stick-breaking construction for the IBP, which renders it amenable to variational inference. Let us consider N observations, and denote as $\mathbf{Z} = [z_{i,k}]_{i,k=1}^{N,K}$ a binary matrix where each entry indicates the existence of feature k in observation i . Taking the infinite limit, $K \rightarrow \infty$, we arrive at the following hierarchical representation for the IBP [23]:

$$u_k \sim \text{Beta}(\alpha, 1) \quad \pi_k = \prod_{i=1}^k u_i \quad z_{ik} \sim \text{Bernoulli}(\pi_k) \quad \forall i$$

Here, $\alpha > 0$ is the innovation parameter of the IBP, which controls the magnitude of the induced sparsity. In practice, $K \rightarrow \infty$ denotes a setting whereby we obtain an overcomplete feature representation of the observed data, that is K equals input dimensionality.

2.2 Stochastic Gradient Variational Bayes

In modern BNNs, inference of the posterior distributions of latent stochastic variables is performed via stochastic gradient maximization of the model evidence lower bound (ELBO). This is commonly referred to as Stochastic Gradient Variational Bayes (SGVB) [24], and requires performing a Monte-Carlo (MC) approximation of the conditional log-likelihood posterior expectations entailed in the expression of the ELBO. As such an approximation results in estimators of prohibitively high variance, one has to resort to some sort of variance reduction technique. A common solution to this end is the reparameterization trick, under which the drawn MC samples are expressed as differentiable transformations of low-variance noise variables ϵ and the parameters of the sought posterior [24]. This is easily attainable when dealing with continuous latent variables, especially of elliptical form, e.g. Gaussians. Yet, it becomes harder when the continuous latent variables we are dealing with are of different form. Specifically, when it comes to models with IBP priors, the entailed Beta-distributed stick variables are not amenable to the reparameterization trick. To address this issue, one can approximate the $\text{Beta}(a_k, b_k)$ -distributed stick variables, u_k , via the Kumaraswamy distribution [25]:

$$p(u_k; a_k, b_k) = a_k b_k u_k^{a_k-1} (1 - u_k^{a_k})^{b_k-1} \quad (1)$$

Samples from this distribution can be reparameterized as follows [26]:

$$u_k = \left(1 - (1 - X)^{\frac{1}{b_k}}\right)^{\frac{1}{a_k}}, \quad X \sim U(0, 1) \quad (2)$$

2.2.1 Dealing with Discrete Latent Variables

In the case of Discrete (Categorical or Bernoulli) latent variables, performing back-propagation through reparameterized drawn samples, as described above, becomes infeasible. Recently, the solution of introducing appropriate continuous relaxations has been proposed by different research teams [27, 28]. Let $\alpha \in (0, \infty)^K$ be the *unnormalized* probabilities of a considered Discrete distribution, $\mathbf{X} = [X_k]_{k=1}^K$, and $\lambda \in (0, \infty)$ be a hyperparameter referred to as the *temperature* of the relaxation. Then, the drawn samples of \mathbf{X} are expressed as differentiable functions of the form:

$$X_k = \frac{\exp(\log \alpha_k + G_k)/\lambda}{\sum_{i=1}^K \exp((\log \alpha_i + G_i)/\lambda)}, \quad G_k = -\log(-\log U_k), \quad U_k \sim \text{Uniform}(0, 1) \quad (3)$$

We set λ as suggested in [28].

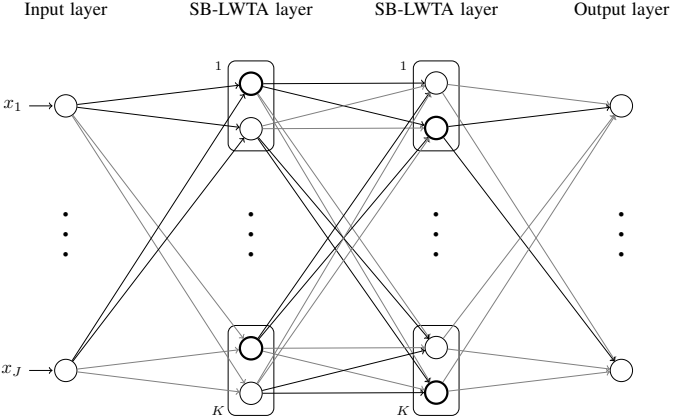


Figure 1: A graphical illustration of the proposed architecture. Bold denotes active units or connections. In our case, we selected $U = 2$ competitors in each LWTA block, $k = 1, \dots, K$.

3 Proposed Approach

In this work, we consider a different paradigm of designing deep networks, where the output of each layer is derived from blocks of competing linear units, and appropriate arguments from nonparametric statistics are employed to infer network component utility in a Bayesian sense. An outline of the envisaged modeling rationale is provided in Fig. 1.

Let $\{\mathbf{x}_n\}_{n=1}^N \in \mathbb{R}^J$ be an input dataset containing N observations, with J features each. Hidden layers in traditional neural networks contain nonlinear units; they are presented with linear combinations of the inputs, obtained via a weights matrix $\mathbf{W} \in \mathbb{R}^{J \times K}$, and produce output vectors $\{\mathbf{y}_n\}_{n=1}^N \in \mathbb{R}^K$ as input to the next layer. In our approach, this mechanism is replaced by the introduction of LWTA blocks in the hidden layers, each containing a set of competing linear units. Layer input components are originally presented to each block as well as each linear unit therein; thus, the weights of the connections are now organized into a three dimensional matrix $\mathbf{W} \in \mathbb{R}^{J \times K \times U}$, where K denotes the number of blocks and U the number of units therein.

Let us consider a layer of the proposed model. Within each block, the linear units compute their activations; then, the block selects one winner unit on the basis of a competitive random sampling procedure we describe next, and sets the rest to zero. This way, we yield a sparse layer output, encoded into the vectors $\{\mathbf{y}_n\}_{n=1}^N \in \mathbb{R}^{K \cdot U}$ that are fed to the next layer. In the following, we encode the outcome of local competition between the units of each block via the discrete latent vectors $\boldsymbol{\xi}_n \in \text{one_hot}(U)^K$, where $\text{one_hot}(U)$ is an one-hot vector with U components. These denote the winning unit out of the U competitors in each of the K blocks of the layer, when presented with the n th datapoint.

To allow for inferring the effective number of (utilized) connections in the layer, we adopt concepts from the field of Bayesian nonparametrics. Specifically, we commence by introducing a matrix of binary latent variables, $\mathbf{Z} \in \{0, 1\}^{J \times K}$; an entry therein is equal to one if the corresponding *set of connections*, $\{w_{j,k,u}\}_{u=1}^U$, is inferred to be of utility to the model, and equal to zero otherwise. Subsequently, we impose an IBP prior over \mathbf{Z} , to allow for performing inference over it, in a way that promotes sparsity, as explained in Section 2.1. Turning to the winner sampling procedure within each LWTA block, we postulate that the latent variables $\boldsymbol{\xi}_n$ are also driven from the layer input, and exploit the model component utility information encoded into the inferred \mathbf{Z} matrices.

Let us begin with defining the expression of layer output, $\mathbf{y} \in \mathbb{R}^{K \cdot U}$. Following the above-prescribed rationale, we have:

$$[\mathbf{y}_n]_{ku} = [\boldsymbol{\xi}_n]_{ku} \sum_{j=1}^J (w_{j,k,u} \cdot z_{j,k}) \cdot [\mathbf{x}_n]_j \in \mathbb{R} \quad (4)$$

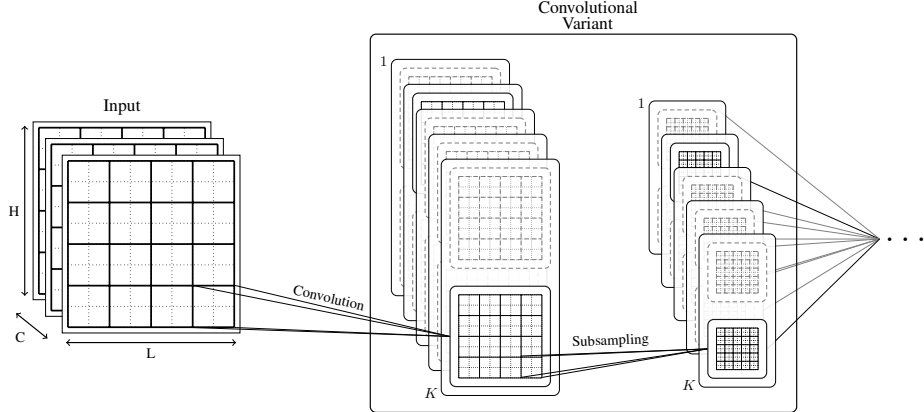


Figure 2: A convolutional variant of our approach. Bold denotes active LWTA feature maps. A kernel (LWTA block) with all its component feature maps deactivated is deemed not of utility, according to the inferred latent indicators z .

where we denote as $[\mathbf{h}]_l$ the l th component of a vector \mathbf{h} . In this expression, we consider that the winner indicator latent vectors are drawn from a Categorical (posterior) distribution of the form:

$$q([\xi_n]_k) = \text{Discrete}\left([\xi_n]_k \middle| \text{softmax}\left(\sum_{j=1}^J [w_{j,k,u}]_{u=1}^U \cdot z_{j,k} \cdot [\mathbf{x}_n]_j\right)\right) \quad (5)$$

where $[w_{j,k,u}]_{u=1}^U$ denotes the vector concatenation of the set $\{w_{j,k,u}\}_{u=1}^U$, and $[\xi_n]_k \in \text{one_hot}(\mathbf{U})$.

On the other hand, the model component utility latent variables, Z , are independently drawn from Bernoulli posteriors that read:

$$q(z_{j,k}) = \text{Bernoulli}(z_{j,k} | \tilde{\pi}_{j,k}) \quad (6)$$

where the $\tilde{\pi}_{j,k}$ are obtained through model training (Section 3.1).

Turning to the prior specification of the model latent variables, we consider a symmetric Discrete prior over the winner unit indicators, $[\xi_n]_k \sim \text{Discrete}(1/U)$, and an IBP prior over the utility indicators:

$$u_k \sim \text{Beta}(\alpha, 1) \quad \pi_k = \prod_{i=1}^k u_i \quad z_{j,k} \sim \text{Bernoulli}(\pi_k) \quad \forall j. \quad (7)$$

Finally, we define a distribution over the weight matrices, \mathbf{W} . To allow for simplicity, we impose a spherical prior $\mathbf{W} \sim \mathcal{N}(\mathbf{0}, 10^{-3}\mathbf{I})$, and seek to infer a posterior distribution $q(\mathbf{W}) = \mathcal{N}(\mathbf{W} | \boldsymbol{\mu}, \text{diag}(\boldsymbol{\sigma}^2))$. This concludes the formulation of a layer of the proposed SB-LWTA model.

Further, we consider a variant of SB-LWTA which allows for accommodating convolutional operations. These are of importance when dealing with signals of 2d structure, e.g. images. To perform a convolution operation over an input tensor $\{\mathbf{X}_n\}_{n=1}^N \in \mathbb{R}^{H \times L \times C}$ at a network layer, we define a set of kernels, each with weights $\mathbf{W}_k \in \mathbb{R}^{h \times l \times c \times U}$, where h, l, c, U are the kernel height, length, number of channels, and number of *competing* feature maps, respectively, and $k \in \{1, \dots, K\}$. Hence, contrary to the grouping of linear units in LWTA blocks within the hidden layers of the network in Fig. 1, the proposed convolutional variant performs local competition among the feature maps of each kernel. That is, each convolutional kernel constitutes an LWTA block. Each layer of our convolutional SB-LWTA networks comprises multiple kernels of competing feature maps each. We consider two competitors in our implementation, without loss of generality.

This way, a layer of the proposed convolutional variant represents an input, \mathbf{X}_n , with a matrix obtained as the concatenation of the *block-sparse* submatrices:

$$[\mathbf{Y}_n]_k = [\xi_n]_k ((\mathbf{W}_k \cdot z_k) \star \mathbf{X}_n) \in \mathbb{R}^{H \times L \times U} \quad (8)$$

where “ \star ” denotes the convolution operation. This may be followed by a pooling procedure to generate the final layer output, as depicted in Fig. 2. Note that, in Eq. (8), local competition among *block feature maps* is implemented via a sampling procedure which is driven from their output, yielding:

$$q([\boldsymbol{\xi}_n]_k) = \text{Discrete} \left([\boldsymbol{\xi}_n]_k \middle| \text{softmax} \left(\sum_{i,j=1}^{H,L} [(\mathbf{W}_k \cdot z_k) \star \mathbf{X}_n]_{i,j} \right) \right) \quad (9)$$

Finally, under this model variant, the utility latent indicator variables, z , are now defined over whole kernels, that is full LWTA blocks. If the inferred posterior, $q(z_k = 1)$, over the k th block is low, then the block is essentially inferred not to be of utility to the network. This essentially induces a data-driven inference procedure over the layer kernels/feature maps.

Our insights motivating this modeling selection concern the resulting computational complexity. Specifically, this formulation allows for completely removing kernels, thus *reducing* the number of executed convolution operations, as per Eqs. (8)-(9). Hence, this construction facilitates efficiency, since convolution is computationally expensive. We postulate the posteriors

$$q(z_k) = \text{Bernoulli}(z_k | \tilde{\pi}_k) \quad (10)$$

with corresponding priors:

$$u_k \sim \text{Beta}(\alpha, 1) \quad \pi_k = \prod_{i=1}^k u_i \quad z_k \sim \text{Bernoulli}(\pi_k) \quad (11)$$

where the $\tilde{\pi}_k$ are obtained through model training (Section 3.1).

3.1 Model Training

To train the proposed model, we resort to maximization of the resulting ELBO expression. Specifically, we adopt SGVB combined with: (i) the standard reparameterization trick for the postulated Gaussian random variables, \mathbf{W} ; and (ii) the Gumbel-Softmax relaxation trick for the introduced latent indicator variables, $\boldsymbol{\xi}$ and z . Under these assumptions, the resulting ELBO of a multilayer SB-LWTA network becomes

$$\begin{aligned} \mathcal{L}(\phi) = \mathbb{E}_{q(\cdot)} [\log p(\mathcal{D} | \{\mathbf{u}, z, \boldsymbol{\xi}, \mathbf{W}\})] - \beta & \left(KL[q(\{z\}) || p(\{z\})] - KL[q(\{\mathbf{u}\}) || p(\{\mathbf{u}\})] \right. \\ & \left. - KL[q(\{\boldsymbol{\xi}\}) || p(\{\boldsymbol{\xi}\})] - KL[q(\{\mathbf{W}\}) || p(\{\mathbf{W}\})] \right) \end{aligned} \quad (12)$$

where we introduce the mean-field assumption across layers, as well as among the latent variables pertaining to different components of the same layer. In this expression, $\beta \in (0, 1]$ is a hyperparameter that controls the contribution of the KL term to model training, \mathcal{D} denotes the training data, and ϕ is the set of the posterior parameters that we seek to learn. For tractability purposes, the posteriors over the stick variables, $q(\mathbf{u})$, are approximated by making use of the Kumaraswamy distribution. At the same time, the posterior expectation of the log-likelihood, as well as the KL terms pertaining to the (relaxed) discrete latent variables, z and $\boldsymbol{\xi}$, are computed by drawing MC samples under the Gumbel-Softmax reparameterization trick [28]. Then, ELBO maximization is performed using standard off-the-shelf, stochastic gradient techniques. In our experiments, we adopt ADAM [29] with default settings.

3.2 Inference Algorithm

Having trained the model posteriors, we can now use them to effect inference for unseen data. In this context, SB-LWTA offers two main advantages over conventional techniques:

(i) By exploiting the inferred component utility latent indicator variables, we can naturally devise a method for removing components that are effectively deemed redundant. To this end, one may introduce a cut-off threshold, τ ; any component with inferred corresponding posterior $q(z)$ below τ is removed from the network. We emphasize that this mechanism is in stark contrast to recent related

work in the field of BNNs; therein, component utility is only implicitly inferred, by thresholding higher-order moments of hierarchical densities over the values of the *network parameters themselves*, \mathbf{W} (see also related discussion in Sec. 1). For instance, [6] recently proposed imposing the following prior over the network weights

$$z \sim p(z) \quad w \sim \mathcal{N}(0, z^2) \quad (13)$$

where $p(z)$ can be a Horseshoe-type or log-uniform prior. It becomes apparent that the interpretation of model component utility under this prior configuration is open to subjectivity. Besides, its very design, especially when it comes to selection of the prior $p(z)$, entails quite an artistry from the side of the practitioners.

(ii) The provision of a full Gaussian posterior distribution over the network weights, \mathbf{W} , offers a natural way of reducing the bit precision level of the network implementation, without affecting predictive performance. Specifically, the posterior variance of the model parameters constitutes a measure of uncertainty in their estimates. Therefore, we can leverage this uncertainty information to assess which bits are significant, and remove the ones which fluctuate too much under approximate posterior sampling. Specifically, we mask the variances, $\mathbb{V}(\mathbf{W})$, with a sample from \mathcal{Z} . Then, the unit round off necessary to represent the weights is computed by making use of the mean of the retained variances, in a fashion similar to [6]. This approach is endowed with the important benefit that the procedure of bit precision selection relies on different posteriors than the component omission process. We posit that by disentangling these two processes we reduce the tendency of the model to underestimate posterior variance. Thus, we may yield stronger network compression while retaining predictive performance.

Finally, let us turn to prediction generation. To be fully Bayesian, we need to sample several different configurations of the random variables in order to assess the predictive density, and perform averaging. This essentially corresponds to sampling several different neural networks, which is inefficient for real-world testing. Thus, we here adopt a common approximation strategy, under which we use the mean of the random variables at inference time, instead of sampling, in a fashion similar to [6, 30].

4 Experimental Evaluation¹

In the following, we evaluate the two proposed variants of our SB-LWTA approach on different benchmarks. We assess the predictive performance of the model and its compression² and pruning effectiveness. We also show that local competition among a limited number of linear units does not undermine performance compared to employing nonlinear units that entail no local competition.

4.1 Implementation Details

Throughout our experiments the stick variables are drawn from a Beta(1, 1) prior. The innovation parameters, α , of the posterior Kumaraswamy distributions of the sticks are initialized at the number of LWTA blocks of their layer; all other initializations are random within the corresponding support sets. The threshold τ is set to 10^{-2} , while the β parameter of the ELBO is set to 10^{-3} . In all our experiments, SB-LWTA networks are evaluated with LWTA blocks that comprise two competitors each. We emphasize that the evaluated simple feedforward SB-LWTA networks remove *connections* on the basis of the corresponding latent indicators z being below the set threshold τ . Analogously, when using the proposed convolutional SB-LWTA architecture, we remove full LWTA *blocks* (convolutional kernels).

4.2 Experimental results

Following the literature, we first consider the classical LeNet-300-100 feedforward architecture. In our SB-LWTA implementation, Lenet-300-100 is split into 150 and 50 LWTA blocks of two competing units, respectively in layers #1 and #2. We evaluate this architecture on the MNIST

¹We have developed our source codes in Python, using TensorFlow [31]

²For calculating the needed bit precision, we use the inferred network weight posterior variances, in a fashion similar to [6]. To this end, we exploit the script provided in: https://github.com/KarenUllrich/Tutorial_BayesianCompressionForDL

Table 1: Learned (Pruned) Feedforward Architectures.

Architecture	Method	Error (%)	# Parameters	Bit precision
LeNet 300-100	Original	1.6	$235K/30K/1K$	—
	StructuredBP	1.7	$23,664/6,120/450$	—
	Sparse-VD	1.92	$58,368/8,208/720$	8/11/14
	BC-GHS	1.8	$26,746/1,204/140$	13/11/10
	SB-LWTA	1.75	$20,262/2,708/113$	3/4/7

dataset. Further, we consider LeNet-5-Caffe³ convolutional net, which we also evaluate on MNIST. The original LeNet-5-Caffe comprises a 5x5 kernel with 20 feature maps on the first layer, a 5x5 kernel with 50 feature maps on the second layer and a dense layer with 500 units on the third. In our SB-LWTA implementation, we consider 10 5x5 kernels (LWTA blocks) on the first layer, and 25 5x5 kernels on the second layer, with 2 competing feature maps each. Finally, we perform experimental evaluations on a more challenging benchmark dataset, namely CIFAR-10 [32]. In this context, we employ the VGG-like architecture⁴ also considered in [6, 30]. Similar to LeNet-5-Caffe, our SB-LWTA implementation of the VGG-like architecture consists in splitting the original architecture into pairs of competing feature maps on each layer.

LeNet-300-100. We train the network from scratch on the MNIST dataset, without using any data augmentation procedure. The obtained comparative results are depicted in Table 1. As we observe, our approach yields competitive accuracy, which is slightly better than the closest related alternative, i.e. BC-GHS [6]. At the same time, our trained network achieves this accuracy competitiveness while retaining the least number of parameters, despite the fact that it was initialized in the same dense fashion as the alternatives. Even more importantly, our method completely outperforms the alternatives when it comes to its final bit precision requirements. These findings vouch for the advantages of inferring discrete latent variables of component utility to effect network pruning, as opposed to the implicit inferential schemes currently adopted in the literature.

LeNet-5-Caffe and VGG-like convolutional architectures. For the LeNet-5-Caffe architecture we do not employ pretrained weights, but we train the network from scratch. In contrast, the considered VGG-like architecture is initially trained with LWTA activations without incorporating the sparsity inducing mechanism; after convergence, we fine-tune the full model to infer component utility and perform network pruning. Our results are presented in Table 2. Since local competition takes place between feature maps, we expect to retain at most the same number of blocks (pairs of feature maps) as the number of feature maps retained by the considered alternatives. In practice, our experimental results show that our approach retains only a fraction of what the alternatives require. In the VGG-like network, our method retains more feature maps in the last layers. However, the total computational complexity is greatly reduced, since more feature maps are dropped in the earlier layers, where convolutions are performed with respect to larger inputs. In addition, our method is significantly more economical in terms of bit precision.

5 Conclusions

We introduced a new design of deep networks, whereby we use biologically inspired local competition-based nonlinearities, driven from a Bayesian inference mechanism. Therein, we employed discrete random variables to assess component utility. This allowed for more effective network pruning compared to the existing paradigm, as well as improved estimation of parameter variance. Hence, we obtained more drastic reduction of bit precision for representing the network weights, with negligible effect in predictive accuracy. As discussed in the Introduction, LWTA-based networks are more potent when it comes to online learning problems, as they are more robust to catastrophic forgetting. Although we have not explored this aspect in this work, we intend to scrutinize these capabilities in real-world settings, as a part of our future research.⁵

³<https://github.com/BVLC/caffe/tree/master/examples/mnist>

⁴<http://torch.ch/blog/2015/07/30/cifar.html>

⁵See Appendix A for some initial investigation of the potency of LWTA activations.

Table 2: Learned (Pruned) Convolutional Architectures.

Architecture	Method	Error (%)	# Feature Maps (Conv. Layers)	Bit precision (All Layers)
LeNet-5-Caffe	Original	0.9	25/50	—
	StructuredBP	0.86	3/18	—
	Sparse-VD	1.0	14/19	13/10/8/12
	BC-GHS	1.0	5/10	10/10/14/13
	SB-LWTA	0.9	6/6	6/3/3/13
VGG-like	Original	8.4	64/64/128/128/256/256/256 512/512/512/512/512/512	—
	BC-GHS	9.0	51/62/125/128/228/129/38 13/9/6/5/6/6/6/20	11/12/9/14/10/8/5/ 5/6/6/8/11/17/10
	SB-LWTA	8.9	50/58/126/124/220/120/36 70/8/6/6/8/30/30/20	10/10/7/10/8/6/5/ 8/7/6/6/9/14/10

References

- [1] Yann LeCun, Yoshua Bengio, and Geoffrey Hinton. Deep learning. *Nature*, 521(7553):436, 2015.
- [2] Yarin Gal and Zoubin Ghahramani. Dropout as a Bayesian approximation: Representing model uncertainty in deep learning. *arXiv:1506.02142*, 2015.
- [3] Jimmy Ba and Rich Caruana. Do deep nets really need to be deep? In *Proc. NIPS* 27, pages 2654–2662. 2014.
- [4] Geoffrey Hinton, Oriol Vinyals, and Jeffrey Dean. Distilling the knowledge in a neural network. In *NIPS Deep Learning and Representation Learning Workshop*, 2015.
- [5] Alex Graves. Practical variational inference for neural networks. In *Proc. NIPS*, pages 2348–2356, 2011.
- [6] Christos Louizos, Karen Ullrich, and Max Welling. Bayesian compression for deep learning. In *Proc. NIPS*, pages 3290–3300, 2017.
- [7] Sotirios Chatzis. Indian buffet process deep generative models for semi-supervised classification. In *IEEE ICASSP*, 2018.
- [8] Hemant Ishwaran and Lancelot F. James. Gibbs sampling methods for stick-breaking priors. *Journal of the American Statistical Association*, 96(453):161–173, 2001.
- [9] Eric R. Kandel, James H. Schwartz, and Thomas M. Jessell, editors. *Principles of Neural Science*. Elsevier, New York, third edition, 1991.
- [10] P. Andersen, G. N. Gross, T. Lomo, and O. Sveen. Participation of inhibitory and excitatory interneurones in the control of hippocampal cortical output. *UCLA Forum Med Sci*, 11:415–465, 1969.
- [11] John C. Eccles, Janos Szentagothai, and Masao Ito. *The cerebellum as a neuronal machine*. Springer-Verlag, 1967.
- [12] C. Stefanis. Interneuronal mechanisms in the cortex. *UCLA Forum Med Sci*, 11:497–526, 1969.
- [13] R. J. Douglas and K. A. Martin. Neuronal circuits of the neocortex. *Annu. Rev. Neurosci.*, 27:419–451, 2004.
- [14] Anders Lansner. Associative memory models: from the cell-assembly theory to biophysically detailed cortex simulations. *Trends in Neurosciences*, 32(3):178 – 186, 2009.
- [15] Daniel D. Lee and H. Sebastian Seung. Learning the parts of objects by nonnegative matrix factorization. *Nature*, 401:788–791, 1999.

- [16] B. A. Olshausen and D. J. Field. Emergence of simple-cell receptive field properties by learning a sparse code for natural images. *Nature*, 381(6583):607–609, Jun 1996.
- [17] Wolfgang Maass. Neural computation with winner-take-all as the only nonlinear operation. In *Proc. NIPS 12*, pages 293–299, Cambridge, MA, USA, 1999. MIT Press.
- [18] W. Maass. On the computational power of winner-take-all. *Neural Comput*, 12(11):2519–2535, Nov 2000.
- [19] Rupesh K Srivastava, Jonathan Masci, Sohrob Kazerounian, Faustino Gomez, and Jürgen Schmidhuber. Compete to compute. In *Proc. NIPS 26*, pages 2310–2318. Curran Associates, Inc., 2013.
- [20] S. Grossberg. The art of adaptive pattern recognition by a self-organizing neural network. *Computer*, pages 77–88, 1988.
- [21] Michael McCloskey and Neal J. Cohen. Catastrophic interference in connectionist networks: The sequential learning problem. volume 24 of *Psychology of Learning and Motivation*, pages 109 – 165. Academic Press, 1989.
- [22] Thomas L. Griffiths and Zoubin Ghahramani. Infinite latent feature models and the indian buffet process. In *Proc. NIPS*, pages 475–482. MIT Press, 2005.
- [23] Y. W. Teh, D. Görür, and Z. Ghahramani. Stick-breaking construction for the Indian buffet process. In *Proc. AISTATS*, volume 11, 2007.
- [24] D. P. Kingma and M. Welling. Auto-encoding variational Bayes. In *Proc. ICLR*, 2014.
- [25] P. Kumaraswamy. A generalized probability density function for double-bounded random processes. *Journal of Hydrology*, 46(1):79 – 88, 1980.
- [26] Eric Nalisnick and Padhraic Smyth. Stick-breaking variational autoencoders. In *Proc. ICLR*, 2016.
- [27] Eric Jang, Shixiang Gu, and Ben Poole. Categorical reparameterization using gumbel-softmax. In *Proc. ICLR*, 2017.
- [28] Chris J. Maddison, Andriy Mnih, and Yee Whye Teh. The concrete distribution: A continuous relaxation of discrete random variables. In *Proc. ICLR*, 2017.
- [29] Diederik P Kingma and Jimmy Ba. Adam: A method for stochastic optimization. *arXiv preprint arXiv:1412.6980*, 2014.
- [30] Kirill Neklyudov, Dmitry Molchanov, Arsenii Ashukha, and Dmitry P Vetrov. Structured bayesian pruning via log-normal multiplicative noise. In *Proc. NIPS 31*, pages 6775–6784. 2017.
- [31] Martín Abadi et al. TensorFlow: Large-scale machine learning on heterogeneous systems, 2015. Software available from tensorflow.org.
- [32] Alex Krizhevsky and George Hinton. Learning multiple layers of features from tiny images. Technical report, 2009.
- [33] Patrice Y. Simard, Dave Steinkraus, and John Platt. Best practices for convolutional neural networks applied to visual document analysis. Institute of Electrical and Electronics Engineers, Inc., August 2003.
- [34] Xavier Glorot, Antoine Bordes, and Yoshua Bengio. Deep sparse rectifier neural networks. In *Proc. AISTATS*, volume 15 of *Proc. of Machine Learning Research*, pages 315–323, Fort Lauderdale, FL, USA, 11–13 Apr 2011. PMLR.
- [35] Geoffrey E. Hinton, Nitish Srivastava, Alex Krizhevsky, Ilya Sutskever, and Ruslan Salakhutdinov. Improving neural networks by preventing co-adaptation of feature detectors. *CoRR*, abs/1207.0580, 2012.

Appendix

A Activations Comparison

In order to assess the efficacy of local competition compared to conventional nonlinearities in deep learning, we perform an experimental evaluation in a similar fashion to [19]. We consider a feed-forward architecture with 3 layers comprising 1000 units per layer for sigmoidal and thresholding activations, and 500 LWTA blocks with 2 units therein per layer for LWTA activations. Additionally, we introduce a softmax layer for classification. We use the MNIST dataset without any data augmentation; pixel values are constrained into $[0, 1]$. Finally, we evaluate SB-LWTA without employing pruning based on the $q(z)$ values, or bit precision reduction based on the posterior variances.

The results of these experiments are presented in Table 3; they suggest that LWTA activations are a powerful and viable biologically inspired alternative to traditional activations. Specifically, our proposed method results in significant compression of the network with negligible effect in predictive accuracy.

Table 3: Different Activations for the considered Feedforward Architecture.

Method	Error (%)	# Parameters	Bit precision
Sigmoid [33]	1.6	784K/1m/1m/10K	—
ReLU [34]	1.43	784K/1m/1m/10K	—
ReLU+Dropout [35]	1.30	784K/1m/1m/10K	—
LWTA-2 [19]	1.28	784K/1m/1m/10K	—
SB-LWTA w/o pruning & compression	1.28	784K/1m/1m/10K	—
SB-LWTA	1.35	240K/500K/360K/2.6K	4/5/4/13

B Beta-Kumaraswamy KL Divergence

Following [26], the KL divergence between a prior $p(u_k) \sim \text{Beta}(\alpha, \beta)$ and a posterior $q(u_k) \sim \text{Kumaraswamy}(a, b)$ reads

$$\begin{aligned} \text{KL}[q(u_k) \parallel p(u_k)] &= \frac{a - \alpha}{a} \left(-\gamma - \Psi(b) - \frac{1}{b} \right) + \log ab + \log B(\alpha, \beta) - \frac{b - 1}{b} \\ &\quad + (\beta - 1)b \sum_{m=1}^{\infty} \frac{1}{m + ab} B\left(\frac{m}{a}, b\right) \end{aligned} \quad (14)$$

where γ is the Euler-Mascheroni constant, $\Psi(\cdot)$ is the digamma function and $B(\cdot)$ is the Beta function.